

Predictability of Coupled Processes

Axel Timmermann

Institute for Marine Research, Düsternbrooker Weg 20, 24105 Kiel, Germany

Abstract: The predictability of coupled multiple-timescale dynamical systems is investigated. New theoretical concepts will be presented and discussed that help to quantify maximal prediction horizons for finite amplitude perturbations as well as optimal perturbation structures. Several examples shall elucidate the applicability of these new methods to seasonal forecasting problems.

1 Introduction:

One of the key elements of all natural sciences is forecasting. In some situations it is the existence of newly predicted particles that decides on the validity of physical theories, in other situations it is the predicted trajectory of a dynamical system that can falsify scientific hypothesis. In the seminal Lorenz (1963) paper, E. Lorenz discovered that certain low-dimensional nonlinear dynamical systems bear an interesting and at that time unexpected property: two initially close trajectories will diverge very quickly in phase space, eliminating the possibility for long-term forecasting. This paper, strongly inspired by the theoretical considerations of Barry Saltzman, gave birth to chaos theory. It is this particular dependence on the initial conditions that is intrinsic to all weather, ocean and climate prediction efforts.

In a uni-timescale chaotic system we have the following situation: The rate of divergence of initially infinitesimally close trajectories can be quantified roughly in terms of the Lyapunov exponent λ that can be expressed in terms of:

$$\lambda = \lim_{t \rightarrow \infty} \lim_{\delta x(0) \rightarrow 0} \frac{1}{t} \ln \frac{\delta x(t)}{\delta x(0)}. \quad (1)$$

With a given error tolerance level of Δ the future state of the system can be predicted T_p ahead, with

$$T_p \sim \frac{1}{\lambda} \ln \left(\frac{\Delta}{\delta} \right). \quad (2)$$

If the dynamical system has different timescales, the Lyapunov exponent is proportional to the smallest characteristic timescale, irrespective of the variance carried by fluctuations on these timescales. On the other hand for geophysical flows predictions can be made far beyond the Lyapunov timescale, that characterizes small scale fluctuations associated with turbulence. In particular for the atmosphere it is the large-scale dynamics that determines long-term predictability (Lorenz 1969). Apparently, the Lyapunov exponent and its association with predictability horizons are of very limited use in multiple time-scale systems. A similar paradoxical situation can occur when we plan to compute the singular vectors for coupled two-timescale systems, such as the coupled atmosphere-ocean system. In order to determine these optimal perturbations using a coupled general circulation model, one needs to compute the Jacobian and its adjoint along the nonlinear phase-space trajectory. An important question is now, what is the associated timescale of the linearized and adjoint coupled models? Do these models really capture the longterm dynamics, associated e.g. with the ENSO phenomenon, or are they mostly capturing the growth of weather perturbations in an adiabatically slow varying oceanic background? Before we dwell into these problems of how to determine optimal perturbation patterns of coupled systems let us return to the concept of Lyapunov exponents.

In an attempt to overcome the difficulties associated with the infinitesimally small amplitude perturbations Aurell et al. (1997) have generalized the Lyapunov exponent concept to non-infinitesimal finite amplitude

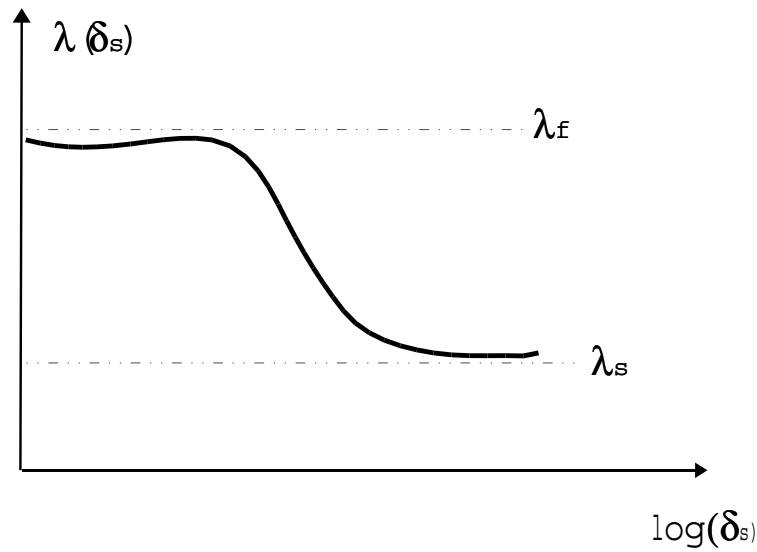


Figure 1: Finite size Lyapunov exponent of two coupled (slow-fast) Lorenz models computed from the slow variables. The two horizontal lines represent the uncoupled Lyapunov exponents. Figure schematized after Bofetta et al. (1998).

perturbations. This generalization has the advantage that both, the nonlinear dynamical evolution of these perturbations as well as the predictability of multiple timescale systems can be treated appropriately (Bofetta et al. 1998). The so-called *finite-size Lyapunov* is defined as

$$\lambda(\delta) = \frac{1}{T_r(\delta)} \ln r, \quad (3)$$

with δ denoting the finite amplitude perturbation of the initial conditions, T_r the time it takes for the initial perturbation to grow by a factor of r . In Bofetta et al. (1998) it is shown that this quantity is a suitable quantity to describe the predictability of multiple-timescale systems. Bofetta et al. (1998) illustrate this new concept by studying the predictability of two coupled sets of nonlinear Lorenz (1963) equations, one characterized by a slow and the other one characterized by a fast time scale. It is shown that for small perturbations $\lambda(\delta)$ is almost equal to the maximum Lyapunov exponent associated with the shortest timescale, whereas for large initial perturbations $\lambda(\delta)$ asymptotically approaches the Lyapunov exponent of the slow decoupled system. This is illustrated in **Figure 1**.

Furthermore, the predictability time T_p of the slow component of the coupled fast-slow Lorenz (1963) system becomes orders of magnitude larger than the one based on the classical Lyapunov estimate, when large error tolerances are allowed for, as illustrated in **Figure 2**.

An interesting example for a coupled slow-fast system, and a challenging one for seasonal forecasters, is the tropical Pacific coupled atmosphere-ocean system with its primary oscillatory instability, the so called El Niño-Southern Oscillation (ENSO) phenomenon. ENSO variability arises from the so-called Bjerknes positive air-sea feedback and a negative feedback provided by slow ocean adjustment processes (Jin 1997). In some ENSO models (e.g. the Zebiak and Cane 1987 model and hybrid coupled models) the atmospheric dynamics is treated in very particular way (e.g. Gill 1980, Kleeman 1991): The linearized atmospheric shallow water equations on

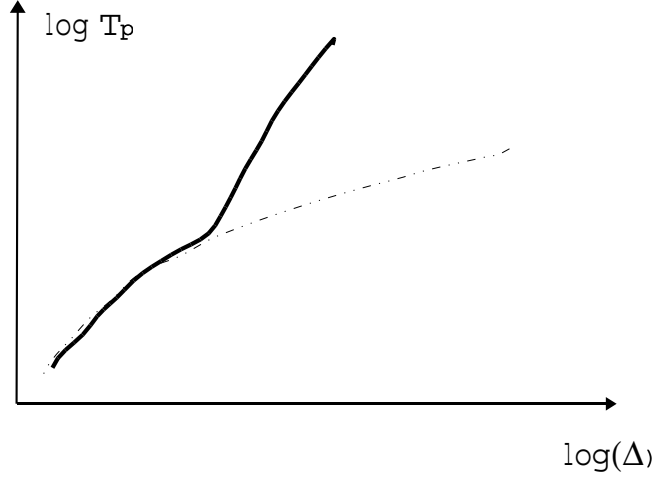


Figure 2: Predictability time for the slow component of the two coupled Lorenz models as a function of error tolerance. The dashed line represents the classical Lyapunov estimate. Figure schematized after Bofetta et al. (1998).

an equatorial β plane for zonal, meridional velocities and the geopotential height anomaly can be written as

$$\frac{\partial u}{\partial t} - \beta y v + \frac{\partial \Phi}{\partial x} = -ru \quad (4)$$

$$\frac{\partial v}{\partial t} + \beta y u + \frac{\partial \Phi}{\partial y} = -rv \quad (5)$$

$$\frac{\partial \Phi}{\partial t} + c_a^2 \left(\frac{\partial u}{\partial x} + \frac{\partial v}{\partial y} \right) = \alpha Q(x, y) - r\Phi. \quad (6)$$

$c_a = 60 \text{ m/s}^2$ represents the equatorial wave speed in the atmosphere. Given a clear timescale separation between atmospheric adjustment and oceanic adjustment, these equations can be simplified such that all acceleration terms are dropped and only the stationary solution (u, v, Φ) for a given diabatic forcing Q is determined. $Q(x, y)$ is a function of the actual SST pattern. This technique, which has been quite successful in studying ENSO dynamics and predictability can be compared with the so-called slaving principle of Haken (1978). Fast variables are assumed to relax very rapidly (or instantaneously) to a state that is a function of the slow variable state vector. This basic principle can be described mathematically as follows: Consider the fast variable x_f that is governed by

$$\frac{dx_f}{dt} = F(x_f, x_s, \zeta(t)) \quad (7)$$

with x_s representing a slow variable, F a nonlinear function and ζ noise with variance Σ . The dynamics of the slow variable is assumed to be given by

$$\frac{dx_s}{dt} = x_f. \quad (8)$$

For illustrative purposes we focus on the simplified system $F(x_f, x_s, \zeta(t)) = -\beta x_f - \frac{dV(x_s)}{dx_s} + \sqrt{2\beta kT} \zeta(t)$. In case of large β one expects a very fast relaxation of the dynamics of x_f towards a quasi-stationary state in which $dx_f/dt \rightarrow 0$. For large enough β , i.e. for quick relaxation times we obtain

$$x_f = -\frac{1}{\beta} \left[\frac{dV(x_s)}{dx_s} - \sqrt{2\beta kT} \zeta(t) \right] \quad (9)$$

Substituting this equation into the dynamical equation (8) yields

$$\frac{dx_s}{dt} = -\frac{1}{\beta} \frac{dV(x_s)}{dx_s} + \sqrt{skT/\beta} \zeta(t). \quad (10)$$

It should be noted here that the order of the stochastic differential equation is reduced by one which might have severe consequences for the dynamics and the predictability. For illustrative purposes let us discuss a climate-relevant example. Locally the heat budget in a fixed mixed layer slab ocean with depth H can be expressed in terms of

$$\frac{dT}{dt} = -\lambda T + \frac{Q}{c_p \rho H}, \quad (11)$$

where T represents the mixed layer temperature and $-\lambda T$ the first term in a Taylor expansion that describes the adjustment of ocean and atmospheric temperatures as well as entrainment processes at the base of the mixed layer. According to Hasselmann (1976) and Frankignoul (1978) Q can be parameterized in high latitudes in terms of stochastic weather fluctuations. Here we choose the following more general ansatz:

$$\frac{dQ}{dt} = -\alpha Q + \sigma \zeta(t) + F_1 T \quad (12)$$

which represents a red noise process and a coupling of the atmospheric fluctuations to the mixed layer temperature. This dependence, parametrizes symbolically the fact that changed meridional temperature gradients have an influence on the eddy momentum transport and heat fluxes in the atmosphere, through changes in baroclinicity. Without adiabatic elimination the equations can be written in terms of a stochastically driven linear oscillator equation.

$$\frac{d^2 T}{dt^2} + (\alpha + \lambda) \frac{dT}{dt} + \left(\alpha \lambda - \frac{F_1}{c_p \rho H} \right) T + \frac{\sigma}{c_p \rho H} \zeta(t) = 0, \quad (13)$$

whereas in the case of adiabatic elimination we obtain the following red noise equation:

$$\frac{dT}{dt} + \left(\lambda - \frac{F_1}{\alpha c_p \rho H} \right) T - \frac{\sigma}{c_p \rho H \alpha} \zeta(t) = 0 \quad (14)$$

The associated spectra look quite differently. The full spectrum of the process exhibits a spectral peak at a particular frequency. This frequency depends mainly on the air-sea coupling F_1 as well as on the damping timescales of the atmosphere and the ocean. The adiabatic elimination does not exhibit any spectral peak. Generally, also the associated prediction times are different. Hence, the usage of the adiabatic elimination has to be done with care, in particular since the order of the differential equations is reduced by one.

This pedagogic example of the adiabatic elimination procedure shall illustrate that a rather straightforward but also "brutal" way of getting rid of the two-timescale problem in predictability studies is to use a quasi-stationarity assumption for the fast variables. This assumption is implicitly made in intermediate and hybrid ENSO prediction models. However, predicting ENSO is more complicated and it has become questionable (Syu and Neelin 2000). The question was raised as to whether fast variables can be really eliminated by slaving principles, or whether they also play a fundamental role in triggering ENSO events. Fast, so-called intraseasonal oscillations in the atmosphere (see **Figure 3**) can kick off Kelvin waves that, under appropriate pre-conditioning of the warm pool, can lead to the onset of El Niño or La Niña events.

Once such oceanic Kelvin waves are triggered, the oceanic evolution is highly predictable to at least a season in advance. Kelvin waves can be compared with a Jack-out-of-the box. Nobody knows exactly when the box is opened, but once it is opened the future is well determined. Of course, this particular feature has strong implications for ENSO prediction, since the predictability time of the individual westerly wind-bursts is very small, whereas the predictability time for the Kelvin wave propagation and the subsequent generation of SST anomalies by local air-sea interactions is much larger. Is there a possibility to overcome the initial uncertainty in predicting westerly windbursts? This is a question of utmost importance since the living conditions of about 30% of the world population are significantly influenced by ENSO related climate anomalies.

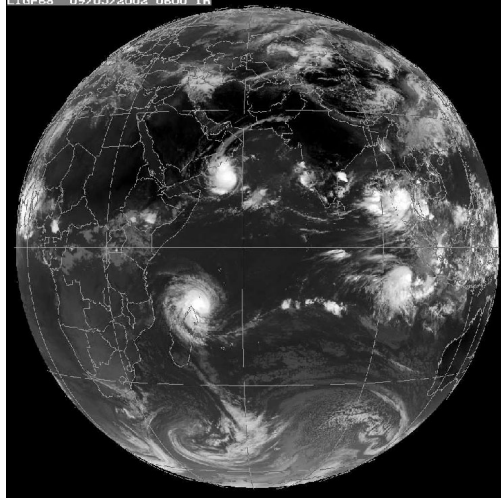


Figure 3: Westery Wind Burst (WWB) over the West Pacific Ocean seen from the satellite in May 2002.

We have already discussed the possibility to eliminate fast fluctuations from the equations of the tropical Pacific coupled atmosphere-ocean system by adiabatic elimination. In a sense the resulting equations can be viewed as a kind of time-averaged set of equations, where only slow oceanic timescales are retained. There are now a few ways to improve on this. One is to take into account the fast fluctuations empirically (see section 2), another way is to derive effective equations of motion directly from the data under consideration (see section 3 and 4).

2 Stochastic Optimals

Tropical Pacific climate variability can be decomposed to a first order into variability Φ associated with the ENSO phenomenon and non-ENSO related stochastic fluctuations θ of variance \mathbf{S} . Anomalies shall be computed with respect to the annual cycle basic state. The stochastically forced dynamical equations for the tropical atmosphere-ocean system can be written symbolically in the form

$$\frac{d\vec{\Phi}}{dt} = \vec{F}(\vec{\Phi}) + \mathbf{S}\vec{\theta} \quad (15)$$

For a Zebiak-Cane type intermediate ENSO model (Zebiak and Cane 1987) the vector $\vec{\Phi}$ might consist of the SST anomalies and the expansion coefficients for the different equatorial wave modes. Given a stable (linearly damped) ENSO mode, this equation can be linearized around a nonlinear trajectory $\vec{\Phi}(t)$. We obtain a dynamical equation for the perturbations (denoted by primes) which reads

$$\frac{d\vec{\Phi}'}{dt} = \frac{\partial \vec{F}}{\partial \vec{\Phi}} \vec{\Phi}'|_{\vec{\Phi}(t)} + \mathbf{S}\vec{\theta}' = \mathbf{A}\vec{\Phi}' + \mathbf{S}\vec{\theta}'. \quad (16)$$

Bold face expressions denote matrices. Integral solutions of this equation can be obtained, once the propagator $\mathbf{R}(\mathbf{t}_1, \mathbf{t}_2) = \mathbf{e}^{\mathbf{A}(\mathbf{t}_2 - \mathbf{t}_1)}$ is known. Then the solutions can be expressed in terms of

$$\vec{\Phi}'(\mathbf{t}_2) = \mathbf{R}(\mathbf{t}_1, \mathbf{t}_2)\vec{\Phi}'(\mathbf{t}_1) + \int_{\mathbf{t}_1}^{\mathbf{t}_2} \mathbf{R}(\mathbf{t}_1, \mathbf{t}_2)\mathbf{S}\vec{\theta}' dt. \quad (17)$$

The first term on the right hand side represents the predictable part of the dynamics, whereas the second part belongs to the unpredictable stochastic part. It is the ratio between these terms that determines the overall predictability of the system (Grötzner et al. 2000) It has been shown by Kleeman and Moore (1997) that the total variance at a given time τ can be obtained from the stochastic forcing terms $\vec{\theta}$ and the so-called stochastic optimals. Assuming Gaussian white noise, the stochastic optimals are the eigenvectors of the operator

$$\mathbf{Z} = \int_{\mathbf{t}_1}^{\mathbf{t}_2} \mathbf{R}^\dagger(\mathbf{t}, \mathbf{t}_1)\mathbf{X}\mathbf{R}(\mathbf{t}, \mathbf{t}_1)d\mathbf{t}, \quad (18)$$

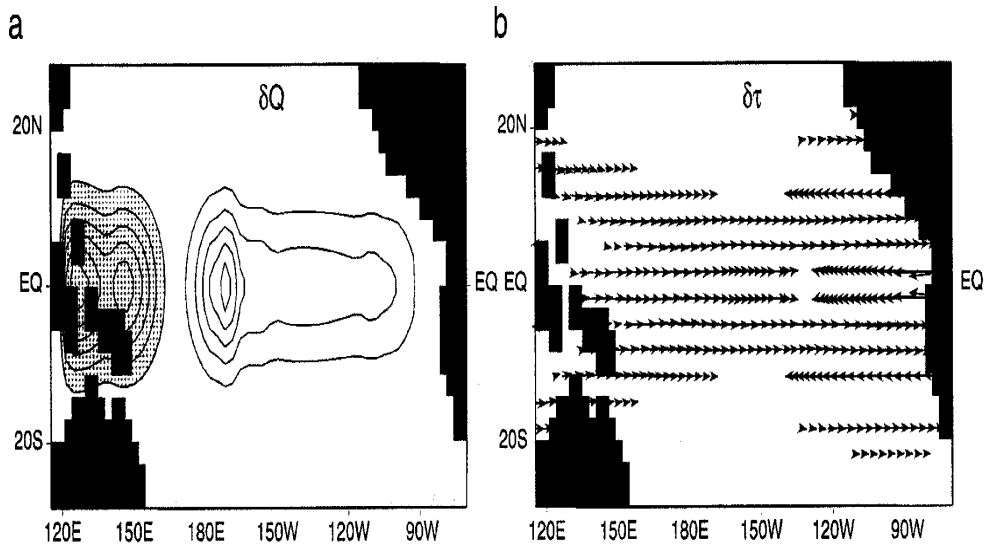


Figure 4: First Stochastic Optimal for heat flux and wind stress anomalies as computed from an intermediate ENSO model. Figure from Moore and Kleeman (1999).

where \mathbf{X} is the kernel defining the variance norm of interest (Farrell and Ioannou 1996). On the other hand the optimal perturbations (singular vectors) (Trefethen et al. 1993) $\vec{\alpha}$ can be computed from the eigenequation

$$\mathbf{R}^\dagger \mathbf{X} \mathbf{R} \vec{\alpha} = \lambda \mathbf{X} \vec{\alpha}. \quad (19)$$

They represent the fastest growing perturbations of the coupled system before nonlinearities become important. The eigenvectors of Z (Stochastic Optimals) corresponding to the maximal eigenvalues are the spatial structures that the stochastic forcing must possess in order to maximize the stochastically induced variance in the model. They are an important quantity for predictability studies of coupled processes. Moore and Kleeman (1999) computed the stochastic optimals for an intermediate ENSO models. The result is shown in **Figure 4**. The heat flux anomalies as well as the wind anomalies are reminiscent of anomalies associated with intraseasonal variability (Hendon and Glick 1997). In fact it turned out (Moore and Kleeman 1999) that the optimal perturbations and stochastic optimals have quite similar structures, indicating that both for initial error growth as well as for the establishment of variance throughout its evolution ENSO is highly sensitive to intraseasonal atmospheric variability. If for a certain time period the atmospheric anomalies do not project well onto the stochastic optimals, the resulting ENSO variance is expected to be small (given a stable ENSO mode). Hence, the pattern of fast atmospheric fluctuations governs the generation of El Niño and La Niña anomalies. It should be emphasized here, that this concept holds only for a stable oscillatory ENSO mode, otherwise the amplitude of ENSO is mainly governed by nonlinearities. This stability assumption is questioned, however, by many climate researchers. At least there is the possibility that ENSO operates close to a Hopf bifurcation point, meaning that ENSO is stable during some decades, whereas it is unstable during other decades. This hybrid hypothesis has been confirmed by the study of An and Jin (2000). In addition to the stability properties of ENSO, Moore and Kleeman (1999) found that also the phase of the annual cycle as well as the nonlinearities and the integrated past noise history are important factors in controlling the sensitivity of ENSO towards stochastic forcing.

Furthermore, it has to be noted here that linear systems can not transfer energy from weather scales to ENSO scales. Hence, the argument that intraseasonal variability forces ENSO is strictly spoken incorrect in a linear framework. What can force ENSO in a stochastic environment are low-frequency variations which probably project onto the patterns of intraseasonal variability. Another possibility is that intraseasonal variability rectifies ENSO through nonlinear interactions. This dilemma has been nicely illustrated in Roulston and Neelin (2001).

3 Nonlinear probabilistic methods

In this section an empirical nonlinear method is described that allows for the determination of optimal perturbation structures associated with low and high predictability. The principal idea of this method is to compute transition probability densities between areas in state space. From these probability densities we learn how quickly certain initial probability density functions are broadened. This dispersion of the probability densities is associated with information loss and hence entropy production. The dispersion rates for different state space elements can be averaged to determine a maximum predictability horizon. The method is closely linked to the empirical derivation of a so-called *Markov Chain*. Let us consider a nonlinear discretized dynamical system

$$x_{t+1} = f(x_t, \zeta_t). \quad (20)$$

ζ_t represents a stochastic component. For simplification the equations are written in univariate form. The generalization to multivariate systems is straightforward. Another way to write down the dynamical equation is given by

$$x_{t+1} = \int dy \delta[x - f(y)] \quad (21)$$

The integrand $\delta[x - f(y)]$ is called Frobenius Perron operator and will be abbreviated by $m(x, y)$. Now all "reasonable" functions $p(x)$ can be written in terms of

$$p(x_{t+1}) = \int dy \delta[x - f(y)] p(y_t). \quad (22)$$

If p belongs to the family of probability density functions, i.e. fulfilling $p \leq 1$ and $\int dy p(y) = 1$ this equation describes how a probability distribution at time t is transformed into a probability distribution at time $t + 1$ under the action of the nonlinear "transition probability kernel" (Frobenius Perron operator) $m(x, y)$. This kernel can be approximated by discretizing the state space of the system into N cells. The state space cells are denoted by x^i and the corresponding probability density by $\vec{p} = (p(x^1), \dots, p(x^i), \dots, p(x^N))$. The evolution equation of the discretized probability density can be written as

$$p^i(t+1) = \sum_{j=1}^N m_t(i, j) p^j(t). \quad (23)$$

It becomes apparent that a good approximation of the Frobenius Perron matrix $m(i, j)$ (transition probability matrix) depends crucially on an intelligent discretization of the state space. Here we use an equi-number (equal-residence time) partition in state space rather than an equi-distant partition of the phase space variables. This partition is shown in **Figure 5** for a one and two dimensional Markov chain.

The advantage of this equi-number partition is that we can exploit some beautiful mathematical properties of the equi-number partition such as the double stochasticity of the transition matrices (meaning that $\sum_i m(i, k) = 1$ and $\sum_k m(i, k) = 1$). The disadvantage is that resolution for extreme state space directions is low. For high dimensional systems the requirements for the amount of available data needed to compute the transition probabilities become very large (Pasmanter and Timmermann 2002). Here we assume that ENSO can be described by relatively few degrees of freedom. In this mathematical context predictability can be easily quantified by the rate in which information about the state of the system is lost - i.e. predictability is associated with the broadening of the probability density. A convenient way of measuring how quickly information is lost is to compute the "distance" between the highly localized initial probability density p_0 and the broadened probability density function at time t using the so-called entropy measure

$$I(t) = \sum_{i=1}^N p^i(t) \ln \frac{p^i(t)}{p_0^i}. \quad (24)$$

Using this equation an averaged loss of information in one time-step can be computed from

$$\langle \Delta I \rangle = -N^{-1} \sum_{i=1}^N \sum_{j=1}^N m(i, j) \ln m(i, j). \quad (25)$$

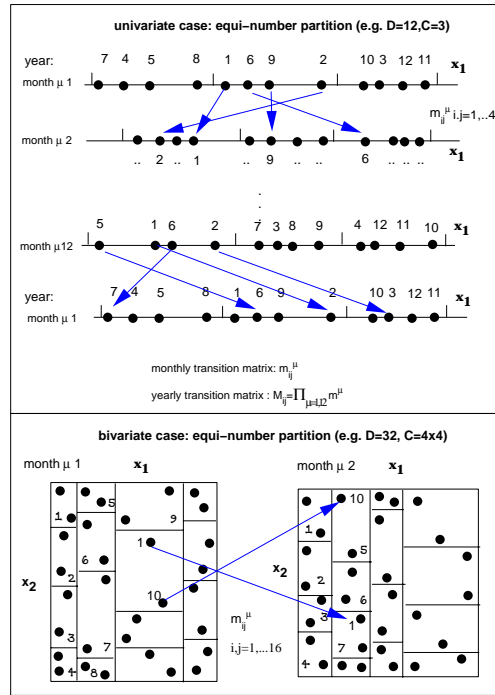


Figure 5: Data partition for the uni-variate and bi-variate cases.

Notice here that the information loss or equivalently the entropy production depends strongly upon the chosen partition. The rate of information loss determines how far ahead we can predict the state of a system, in other words when the probability density becomes too broad, the state of the system is becoming less and less defined. We can compute entropy production for all possible initial conditions in state space, denoted by the cell number j . An interesting problem is to find the initial conditions $\delta_{j,k}$ that are associated with the largest entropy production for a given forecast time τ . These physical initial conditions expressed in terms of a localized δ function in probability space are associated with the eigenvectors of the Markov transition matrices. Since each cell number corresponds to an N -dimensional vector in physical space, we can compute those initial structures that are associated with the slowest or the largest entropy production for a given lead time τ . Using this method, optimal initial perturbations can be determined empirically for a nonlinear coupled system, given a long multivariate dataset that covers the state space densely enough. This method is applied to a 640-year long simulation of the intermediate ENSO model developed by Zebiak and Cane (1987). **Figure 6** depicts the simulated Niño 3 SSTA index. As can be seen from this timeseries, the tropical Pacific atmosphere ocean system seems to operate in regimes: an interannual ENSO regime and a quasi-annual regime that is characterized by westward propagating anomalies. Both regimes alternate chaotically. It can be shown that without a seasonal cycle forcing, the Zebiak and Cane (1987) ENSO model exhibits type-III intermittency.

Our goal here is to determine those oceanic initial conditions that are associated with the fastest loss of information. A two-dimensional cyclic Markov chain is constructed from the leading two EOFs and the corresponding principal components of the simulated monthly thermocline depth anomalies¹. An equi-number partition of the state-space spanned by the first two principal components is chosen and the annual cyclostationarity of the climatic background state is taken into account by an extension of the Markov chain method to cyclostationary nonlinear processes (Pasmanter and Timmermann 2002). **Figure 7** shows the entropy production for different seasons averaged over all initial conditions. We observe a relatively fast entropy growth, and hence a low predictability, during the spring season as compared to autumn and winter season. This well-known feature of the

¹Fast weather variables are neglected in the model formulation. The atmospheric fields are computed from the stationary Gill (1980) model. However, the technique is also applicable to ENSO models that resolve fast atmospheric processes as well as slow oceanic processes.

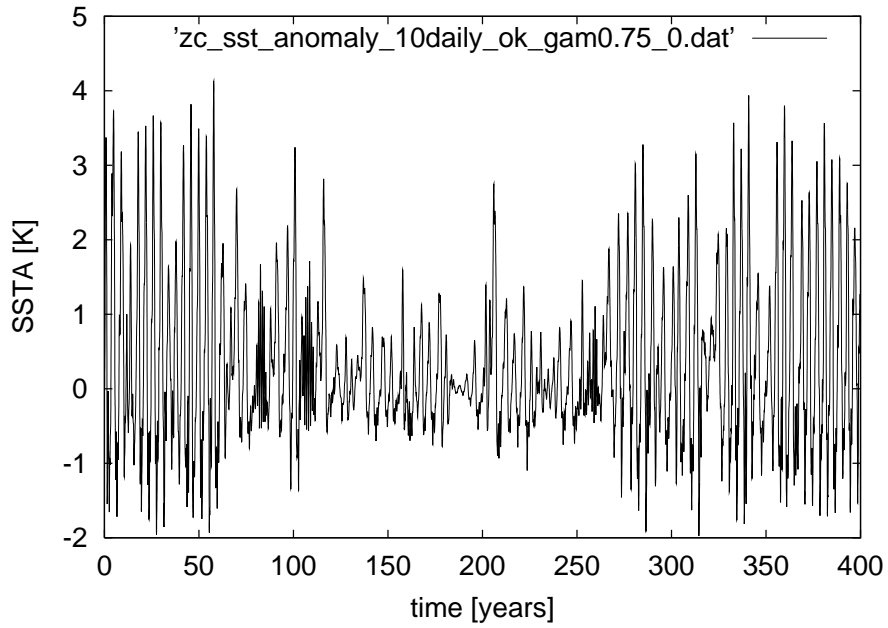


Figure 6: Niño 3 SST anomalies simulated by the Zebiak and Cane (1987) model using the standard configuration of parameters.

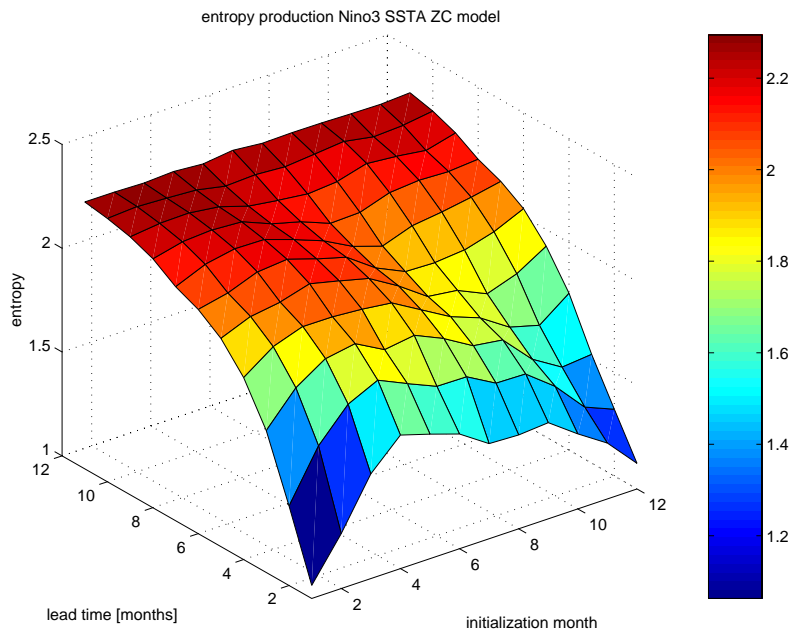


Figure 7: Seasonal dependence of the entropy production: Entropy as a function lead time and of the initialization month.

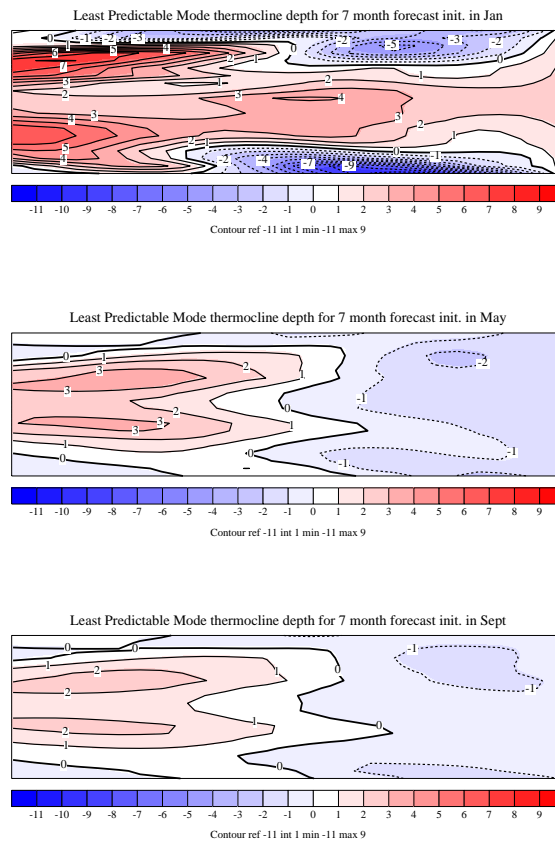


Figure 8: Most unpredictable thermocline depth anomaly patterns for a 7 month forecast initialized in January, May and September.

so-called spring barrier has puzzled many researchers and is still a major obstacle for long-lead ENSO forecasting. It can be partly attributed to the seasonally varying atmosphere-ocean instability, that attains largest values in spring and that contributes also to the phase-locking of ENSO to the annual cycle.

In the next step we calculate those seasonally varying thermocline depth anomaly patterns that are associated with the strongest entropy production for a given lead time of 7 months. The result is depicted in **Figure 8**. The so-called MUM patterns (Most Unpredictable Mode) for a forecast initialized in May and in September are associated with an anomalously deep warm pool, corresponding to the situation when downwelling Rossby waves "hit" the west Pacific boundary. Such a situation can easily generate a downwelling Kelvin wave pulse due to Rossby-Kelvin wave reflection at the western boundary. However, the fate of this Kelvin wave and its potential to amplify into an El Niño event depend very much on the seasonally varying atmosphere-ocean instability. The MUM pattern determined here is similar to the singular vectors determined for the ZC model (Chen et al. 1995) and other intermediate ENSO models (Moore and Kleeman 1997, and Eckert 1999). A very helpful diagnostic for ENSO forecasting would be a number that characterizes how much the present observed state of the tropical Pacific resembles the MUMs. This would provide additional information on the quality of the forecast at the moment of model forecast.

We suggest the following methodology:

- Compute MUMs empirically for a number of intermediate ENSO models and complex Coupled General Circulation Models using multivariate cyclic Markov chains and different state-space partitioning techniques.
- Assess their robustness in space and time

- Project the observed oceanic and atmospheric state onto the MUMs using a reasonable norm.

The resulting numbers contain important information on the potential predictability associated with the initial conditions. Of course this number is furthermore obscured by model uncertainties and caveats that we have not taken into account here. In this section we have discussed how to deal empirically with the longterm predictability of coupled processes, without considering the fast timescale explicitly.

4 Nonlinear deterministic methods

This section describes a relatively new method (Breiman and Friedman 1985, Timmermann et al. 2001) that allows for the empirical extraction of equations of motions from data. Let us begin with the "mother" deterministic dynamical system, prognosing the variables x_j .

$$\dot{x}_i = F_i(\vec{x}) \quad (26)$$

The question arises now, is it possible to reconstruct the "mother" function F from the data x_j under consideration. This is a very difficult task and requires large amounts of data. A simple trick however facilitates the reconstruction enormously. If the dynamical equations can be written in terms of a sum of nonlinear functions

$$\dot{x}_i = \sum_j \Phi_i^j(x_j) + \text{Residual} \quad (27)$$

the functions $\Phi_i^j(x_j)$ can be determined statistically by performing a multiple non-parametric regression analysis between the variables x_j and their numerically computed derivatives. This multiple non-parametric regression exercise can be solved by using the so-called Alternating Conditional Expectation (ACE) Value algorithm. This iterative technique that provides lookup tables for the estimated functions $\tilde{\Phi}_i^j(x_j)$ was developed by Breiman and Friedman (1985). It was applied for the first time in a climate context by Timmermann et al. (2001).

It works as follows:

The ACE algorithm converges in a consistent way to optimal transformations as has been shown by Breiman and Friedman (1985). For details on the numerical implementation of the ACE algorithm see ref. (Voss 2001, Voss and Kurths 1997) The modified ACE algorithm works as follows: Globally optimal solutions (in a least square sense, i.e., $\langle (\dot{x}^j - \sum_{i=1} \tilde{\Phi}_i^j(x^i))^2 \rangle = \min$) can be obtained iteratively from the sequence

$$\tilde{\Phi}_{i,0}^j(x^i) = \langle \dot{x}^j | x^i \rangle, \quad (28)$$

$$\tilde{\Phi}_{i,k}^j(x^i) = \left\langle \dot{x}^j - \sum_{p \neq i} \tilde{\Phi}_{p,k^*}^j(x^p) \middle| x^i \right\rangle. \quad (29)$$

The index j corresponds to the component of the differential equation, k to the iteration step ($k > 0$) and p to the sum over the predictor components. The index k^* equals k for $p < i$ and $k - 1$ for $p > i$, and $\langle .. | .. \rangle$ denotes the conditional expectation value. The so-called optimal transformations $\tilde{\Phi}_{i,k}^j(x^i)$ produced by this algorithm are given in the form of numerical tables. In the expression (29) only scalar quantities are involved, and in contrast to Eq. (26) only one-dimensional conditional probabilities (or, equivalently, two-dimensional joint probabilities) have to be estimated. These can be interpreted in terms of the time transition probabilities or as the dynamical contribution to the componentwise Frobenius Perron operator of the underlying dynamical system.

Minimizing $\langle (\dot{x}^j - \sum_{i=1} \Phi_i^j(x^i))^2 \rangle$ is equivalent to the maximization of the correlation

$$\Psi(\dot{x}^j, x^1, \dots, x^N) = \frac{\langle \dot{x}^j \sum_i \tilde{\Phi}_i^j(x^i) \rangle}{(\langle \dot{x}^{j2} \rangle \langle [\sum_i \tilde{\Phi}_i^j(x^i)]^2 \rangle)^{1/2}}, \quad (30)$$

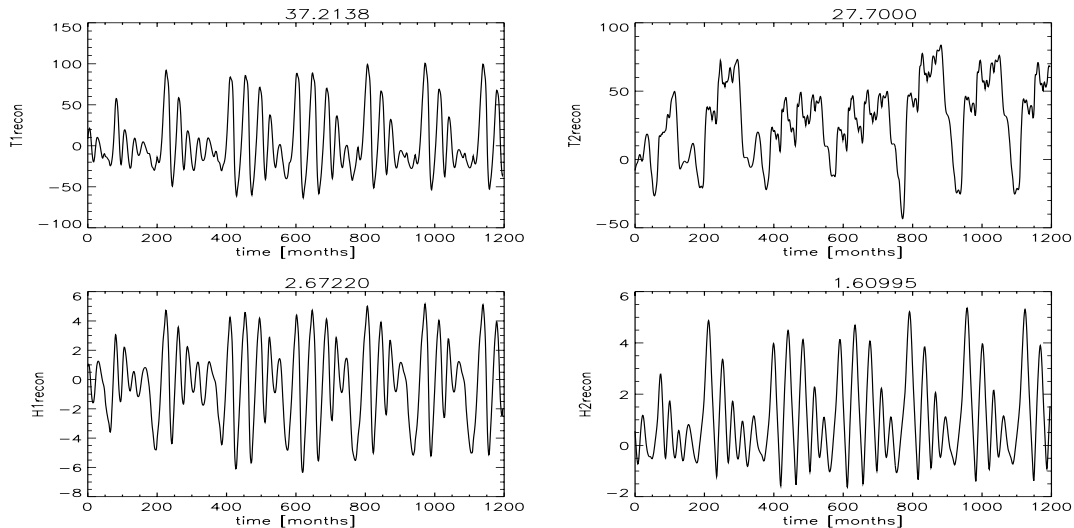


Figure 9: Simulated principal components for the two leading temperature and sea level anomaly EOFs. The simulation is based on a 4-dimensional nonlinear ENSO model that has been derived empirically from a CGCM simulation (Timmermann et al. 2001) using non-parametric multiple regression techniques.

where it is assumed that all variables have zero mean. Hence, this technique to solve the nonlinear regression problem is also called maximal correlation approach.

Once derived empirically, the functions $\Phi_i^j(x_j)$ can be used in order to build a numerical (forecasting) model for the variables under consideration. It is useful to concentrate a priori on a set of dynamically relevant variables. Here, we show how this empirical nonlinear technique can be applied to the ENSO prediction problem. We used a 240-year-long climate simulation performed with the Coupled General Circulation Model (CGCM) ECHAM4/OPYC3 (Timmermann et al. 1999). The simulated ENSO activity (pattern, phase-locking, amplitude) is quite realistic, although the frequency of the simulated ENSO is somewhat too short (2.3 years). We performed an EOF analysis of the simulated sea level depth anomalies (in a 1.5 layer model equivalent to thermocline depth anomalies) as well as of the SST anomalies. According to the recharge oscillator concept for ENSO (Jin 1997), these two variables are key variables to explain ENSO. The leading principal components of two SST (T_1, T_2) and two sea level EOFs (H_1, H_2) were taken, their derivatives were computed and the ACE algorithm was applied to these variable pairs. For computational convenience the resulting functions $\Phi_i^j(x_j)$ were fitted by higher order polynomials and the resulting ordinary differential equation system was integrated in time using a Runge Kutta scheme of 4th order. As can be seen from **Figure 9** the principal components simulated by this 4-dimensional nonlinear low order ENSO model captures most essential features of the CGCM ENSO. An interesting reconstructed feature is that ENSO exhibits decadal amplitude modulations. These decadal amplitude modulations of ENSO can be explained by the theory of homoclinic orbits (Timmermann 2002). How can such a reduced dynamical model be used in order to assess the predictability of ENSO?

This empirical model, that was derived from monthly anomalies, captures the dynamics of effective, averaged variables. Short weather fluctuations are not explicitly resolved, but their effect on the dynamics of ENSO is captured empirically. The full CGCM model is far too complex to compute optimal perturbations for ensemble prediction experiments. Besides, the above-mentioned problem of fast-slow timescale systems prevents a straight-forward linearization of the coupled atmosphere-ocean model code and the computation of its adjoint. The simplified ENSO model however, based on the simulated dynamics of the CGCM can be linearized around its nonlinear trajectory, by a Taylor expansion of the functions $\Phi_i^j(x_j)$. The resulting 4x4 matrix can be transposed and singular vectors can be determined for any given lead time. The same procedure can be performed for different variables for higher dimensional systems and different "mother" CGCMs. If the resulting optimal perturbations are robust with respect to reasonable changes in the dimensions etc, these patterns can be used in

order to perturb the CGCM in seasonal forecasting ensemble simulations. Also here, empirical modeling might help to circumvent the multiple-timescale problem sketched in the introduction.

5 Beyond Error growth: Predictability of the third kind

In weather and climate prediction we distinguish two different types of prediction (Lorenz 1975).

- Predictability of the first kind characterizes initial value problems, exemplified by conventional weather forecasting practice. It measures how uncertainties in the initial conditions evolve during the forecasting period. Different techniques such as the breeding vector and the singular vector techniques, have been developed that help to find those initial perturbations, that are associated with the maximal growth of initial errors with respect to an a priori chosen norm.
- By contrast, for predictions of the second kind, an attempt is made to forecast how a system will respond to prescribed changes in its determining parameters. The response of the climate system to a doubling of the atmospheric carbon dioxide concentrations is a famous example.

An important question arises now: Is there a possibility to determine the state of a nonlinear dynamical system beyond error growth timescales, even when the external "parameter" forcing is constant? And if yes, can we exploit this kind of information for long-term forecasting. The answer to this question is a preliminary yes. Owing to nonlinearities, certain chaotic systems possess global phase-space topologies that can be exploited using statistical techniques. The following system of equations which constitutes the normal form of a triple instability (Arnéodo et al. 1991) and which describes the dynamics of the chemical Belousov-Zhabotinsky reaction is a suitable and illustrative example. The dynamical equations are:

$$\dot{x} = y \quad (31)$$

$$\dot{y} = z \quad (32)$$

$$\dot{z} = -\eta z - \nu y - \mu x - k_1 x^2 - k_2 y^2 - k_3 xy - k_4 xz - k_5 x^2 y \quad (33)$$

with $k_1 = -1, k_2 = 1.425, k_3 = 0, k_4 = -0.2, k_5 = 0.01, \eta = 1, \mu = 1.38, \nu = 1.3$. The dynamics is shown in **Figure 10**.

We observe a fast chaotic oscillation with a period of a few time steps and a peculiar bursting behaviour with a much longer timescale (50-100 timesteps). The phase space view of the system illustrates that the trajectory spirals out of the neighborhood of a saddle node and returns to it via a large amplitude excursion. This kind of behaviour is reminiscent of homoclinic dynamics. In fact our parameter values are chosen such that the system operates close to a homoclinic orbit. Due to the strong skewness of the probability distribution of the variable x large amplitude excursions become less likely for large x values. As expected for such a skewed probability distribution, the averaged return times of large negative excursions grow with the size of the excursions. What is however peculiar for this system, in contrast to skewed white noise, is that there are lower bounds of return times, in particular for large amplitude bursting events. The reason is the global topology of the attractor that follows the shadow of a homoclinic orbit. The system, after a large negative excursion has to return to the neighborhood of the saddle node, spiral around it a couple of times before a new extremum of x can be attained. There are now several interesting questions which can be addressed:

- If there was a bursting event n timesteps back, what is the probability of occurrence for a similar event, m timesteps ahead?
- If the distance between the last two observed bursting events was n timesteps, what is the probability that the next bursting events are separated by m timesteps?
- Are there forbidden return times of extreme events?

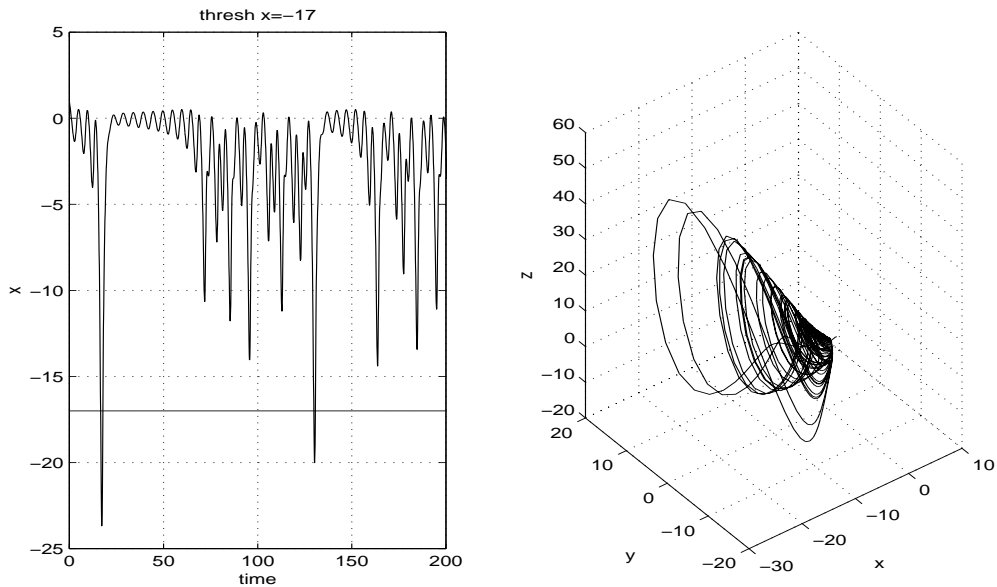


Figure 10: Left: time series of the x -variable of the triple instability dynamical system. A threshold level of $x=-17$ is indicated. Right: Phase-space plot (x,y,z) of the dynamical equation. The underlying dynamical system is believed to capture important dynamics of the chemical Belousov-Zhabotinsky reaction.



Figure 11: Nonlinear wave structures generated by the Belousov-Zhabotinsky reaction that can be described in terms of the dynamical equations of a triple instability.

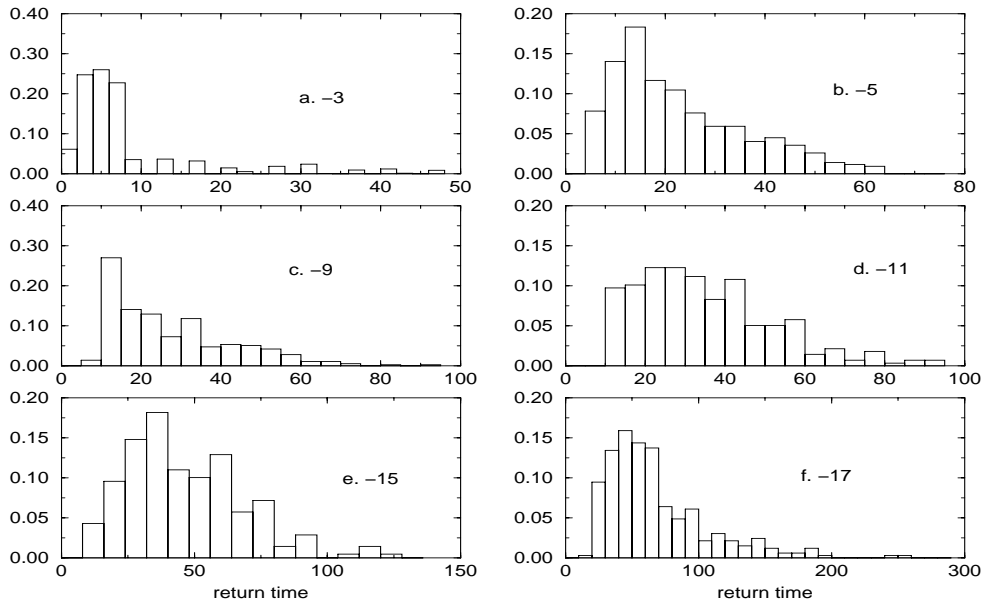


Figure 12: Histogram of the return times of bursting events that exceed different threshold levels. Note the different x -scales

- If yes, what is the dynamical (physical) reason for such forbidden return times?

Let us assume for a moment, that a "bursting event" stands e.g. for a very strong El Niño event. It is obvious in this case that answers to these questions would be of outmost importance and are beyond the reach of "classical" ENSO prediction schemes. In order to address the first question we have computed the probability of the return time for several threshold values in x . The result for the triple instability system is shown in **Figure 12**.

Clearly we see something like "forbidden return times" for large amplitude events and a shift towards larger return times for larger negative x excursions. Note, that we are not predicting the next bursting event deterministically, but, owing to the nonlinearity of the dynamical system, we can assess the risk of extreme events, statistically. The second question can be addressed by computing the conditional probability distributions for previous and future extreme event occurrences. It is the probability that, given the last time interval between two extreme events was τ_1 , the next extreme event will occur τ_2 from the previous one. We computed such a conditional probability distribution for the triple instability dynamical system. The result is depicted in **Figure 13**.

In order to see the fundamental differences that arise from the global topology of the attractor, the resulting figure (**Figure 13**) can be compared with that of a stochastic process, based on a suitable statistical/physical null hypothesis. Let us dream what this might imply for ENSO prediction: Our assumption here is that we know the conditional probability of the return times for the real ENSO system. The distance between the last very large events was 15 years (1982,1997). With a map similar to the one in **Figure 13** we would be able to tell that the next comparable event will occur within the next 8 years with a probability of say 10%, within the next 10 years with a probability of say 35% and within the next 20 years with a probability of say 80%. However, no one (except for the Laplacian demon) possesses such a map for the real ENSO system and it might be obscured by weather noise. Such return time maps can be computed for any system (even for stochastically forced systems). However, most interesting information can be expected for systems that exhibit deterministic bursting behaviour, such as systems that operate in the parameter vicinity of a homoclinic or heteroclinic connection.

Using a low-dimensional nonlinear dynamical system we have shown that predictive information can be extracted from the system far beyond the typical growth timescales associated with initial condition errors. Our approach exploits the bursting behaviour of certain dynamical systems. We suggested a new kind of predictability (the so-called *third kind of predictability*) which is based on the global properties of the attractor, rather than on the local properties (such as for the first kind of predictability).

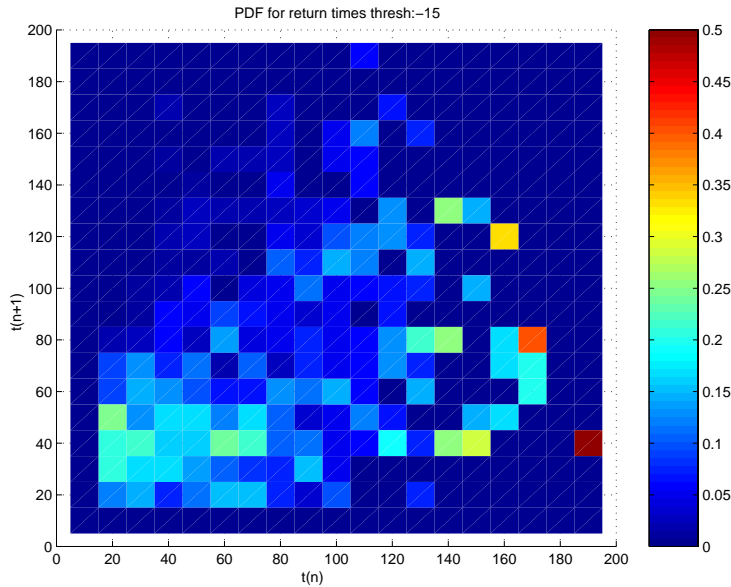


Figure 13: Conditional probability spectrum for return times of threshold exceedances using a value of $x < -15$.

Inspired by these considerations, let us ask the question: Is there any example in climate research for which we can exploit this kind of global predictability? The answer is: maybe. It is well known that ENSO exhibits amplitude modulations on a decadal timescale. Large El Niño events do not occur in a close sequence. There seems to be a certain systematics in their return, which can be explained physically using e.g. the nonlinear recharge model (Timmermann et al. 2002). In fact it can be shown (Timmermann 2002) that several ENSO models of different complexity exhibit bursting behaviour similar to the observations and that is due to the presence of homoclinic or heteroclinic connections between stationary points. A proof, however, that the real tropical Pacific climate system falls into this category, has not been formulated yet. The following considerations are very preliminary, but they might help to illustrate the philosophy of our approach. **Figure 14 b** depicts the observed eastern equatorial Pacific SST anomaly timeseries and its smoothed interannual wavelet energy. Computing the wavelet energy is a means to obtain a timeseries that represents the envelope of the original SSTA timeseries. We clearly observe that eras of high ENSO variance alternate with eras of low ENSO variance on a decadal timescale. If the physical mechanism for these amplitude modulations is similar to the one found in different ENSO models (Timmermann 2002, Timmermann et al. 2002), we sense the temptation to predict the next high ENSO variance era, maybe 10 years ahead.

In order to predict the evolution of ENSO variance we fit polynomials (Hegger et al. 1999, Casdagli, 1989) to the embedded tendency time series of simulated and observed ENSO variance (Figures 14 a and b). The respective estimated dynamical model is used to make out-of-sample forecasts. For the CGCM simulation an embedding dimension of 3 and a delay of 48 months is used. For the observations we choose a delay of 36 months. The ten year lead anomaly correlation skill (not shown) obtained for the envelope curves shown in Figures 14 a and b is about 0.8 and 0.6, respectively. Motivated by this result we perform a real forecast of the next ENSO regime. Our prediction for the envelope curve of ENSO is shown in **Figure 14 b** (blue). According to our forecasting procedure an increase of ENSO variability is expected in the coming decade.

It has to be noted here that there is no physical justification for the mathematical ansatz chosen here other than the idea that ENSO bursting is governed by nonlinear dynamics.

What has not been taken into consideration here is how errors in the estimation of the wavelet variance that naturally emerge due to the shadowing effect of continuous wavelets (Torrence and Compo 1999) affect the forecasts of the envelope. The associated question is, how good can we estimate the interannual wavelet variance of ENSO on September, 12th 2002. Different estimates can be obtained with different buffering techniques of the future timeseries such as zero-tapering or AR(2) surrogates (Timmermann et al. 1999a). According to this "illustrative" forecast, the positive trend increases and a super ENSO regime is predicted for the coming

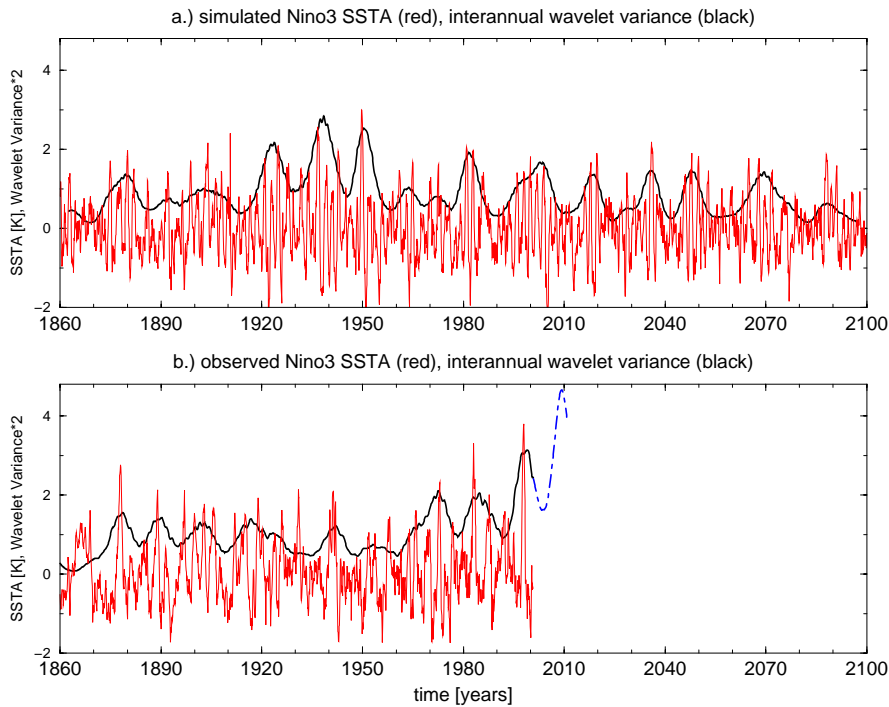


Figure 14: a. Niño 3 SSTA simulated by the ECHAM4/OPYC3 model (red) and its interannual wavelet energy (black). b. Observed Niño3 SSTA time series (red) and its interannual wavelet energy (black), 10 year forecast of interannual wavelet energy (blue) using nonlinear prediction techniques.

8-10 years. A possibility to improve on this deterministic forecasting ansatz is to take into account the errors in estimating the initial ENSO variance, errors in estimating the right coefficients in the fitted 3-d polynomial as well as the small sample size (140 years of monthly data). With these refinements, it will be possible to make Monte Carlo ensemble forecasts, which will yield probabilities for the next very active ENSO regime to occur in say 5-10 years. These very preliminary results are presented here in order to illustrate the methodology and to document that predictive information might be contained in the bursting behaviour of certain dynamical systems, that has not been exploited yet for seasonal forecasting purposes.

6 Some remarks on ENSO prediction models

If we take a look into the *COLA Experimental long lead forecast bulletin* (<http://grads.iges.org/ellfb>) we will find many statistical ENSO prediction models and as has been shown by Landsea (2001) these statistical models that can be run on PCs can compete with the most sophisticated numerical coupled atmosphere-ocean models used in seasonal forecasting (e.g. Stockdale et al. 1998). However, it has to be noted here, that the statistical models predict only indicators such as the Southern Oscillation index or the Niño 3 SSTA index and not the full weather patterns and their ENSO-related changes. Why are these simple models, which are based on a few lines of fortran code and a random number generator so successful in predicting ENSO indicators? Are the sophisticated numerical models just expensive but physically consistent random number generators? Do we really need to resolve global small scale weather patterns, in order to predict ENSO? It is obvious that the timing and amplitude of individual westerly wind bursts (WWBs), kicking off oceanic Kelvin waves that might initiate an El Niño or a La Niña event cannot be predicted 6 months ahead neither by coupled atmosphere-ocean models nor by statistical models, which do not take into account WWBs explicitly. Hence, in both cases long-term ENSO prediction is hampered by the difficulty in predicting individual westerly wind bursts. The predictable part of e.g. an El Niño event is mainly due to the Jack-out-of-the-Box part associated with the

Kelvin wave propagation plus the SST adjustment part and the slow discharging of the equatorial heat content due to the zonally integrated Sverdrup transport. An important question is now, do we really need to resolve atmospheric weather patterns, oceanic instability waves and day-and-night cycles in order predict the warming of the eastern equatorial Pacific several months or seasons ahead? Let us assume, we have a perfect model formulated in terms of nonlinear partial differential equations (PDE) and a very bright *mathematician* who is capable of averaging these PDEs in time analytically. The result would be a new set of averaged equations $\frac{1}{T} \int_0^T dt \text{PDE}(t)$. Now let us assume, we have a perfect model based on the original PDEs that simulates ENSO most realistically and a clever *statistician* who instead of averaging the equations averages the ensemble output of the model. Based on the central limit theorem and assuming independent variables he would argue that the distributions of the simulated variables would approach a Gaussian distribution for longer averaging periods. The longer the averaging period, the more linear the process appears to be. The statistician would be able to derive a quasi-linear model from the simulated data. It would in fact be surprising if the *mathematician* and the *statistician* obtain very different results. Hence, it appears that the key for the success of linear statistical ENSO prediction schemes is the central limit theorem. Averaging reduces the noise but still basic features of the ENSO mode are retained (see eq.(17)). There is however, one important statistical feature that cannot be captured by linear statistical models that operate on a monthly basis, the skewness of the observed monthly Niño 3 SST probability distribution (Burgers and Stephenson 2001). The role of the nonlinear temperature advection in generating this skewed probability distribution has been explained by Jin et al. (2002). It is in particular this nonlinearity that is associated also with the propagation characteristics of SST anomalies that determines the occurrence of very large El Niño events. This skewness cannot be captured by linear statistical models, and hence they exhibit errors in the amplitude either of El Niño or La Niña events.

We have seen that both numerical ENSO models as well as statistical models have some value in predicting ENSO anomalies several months ahead. Unfortunately the advantages of these two modeling philosophies are rarely combined. Despite of the fact that the success of combined multi-model forecasts is well documented (Metzger et al. 2002) only few examples exist where weather and climate prediction centers employ both approaches in an optimal way (see Krishnamurti's talk). The idea of a combined multimodel-ensemble (superensemble) forecast is simple: Let us assume we have N ENSO prediction models, denoted by $M_i, i \in \{1, \dots, N\}$, each providing a 6 month forecast say for the Niño 3 SSTA index X_t . The basic idea of combined forecasts is to find an optimal linear-combination such that residual errors with respect to the observations and an a priori chosen norm are minimized. The optimal forecast is obtained from $X = \sum_{i=1, N} \alpha_i X_i(M_i)$. Basically the models are weighted by their hind- and/or forecast skills. This strategy can be refined in many ways. One is to take into account also the time-derivatives, another is to choose the α_i in such a way that they dependent on the physical situation, representing the fact that some models work well e.g. for a basic state that favors westward-propagating SST anomalies, others perform well for eastward-propagating anomalies etc. Hence, with very little statistical efforts (one just has to compute a multiple linear regression) it would be easy to improve ENSO forecasts. I think it is time now to come up with a combined multi-model ensemble climate community ENSO forecast that adds extra value to the zoo of existing forecasts because it can compensate the weaknesses of some models by the strengths of other models, depending on the existing situation in the tropical Pacific.

Let me finish this section by one last remark on the statistical assessment of seasonal forecasts: The value of an ENSO prediction model is often measured by the difference between the anomaly correlation skill (or r.m.s) of the model under consideration and a damped persistence forecast. Why do we choose a damped persistence forecast, that corresponds to a red noise process, if ENSO is an oscillatory mode? In fact if the performance of the ENSO prediction model is tested against a physically more justified null hypothesis, such as a noise driven oscillator, the difference between model anomaly correlation skill and AR(2) anomaly correlation skill would be even less, as shown by Burgers (2000).

SIO/MPI HCM-T3.0 Tropical SST Anomaly Forecast, 04 Jun 2002

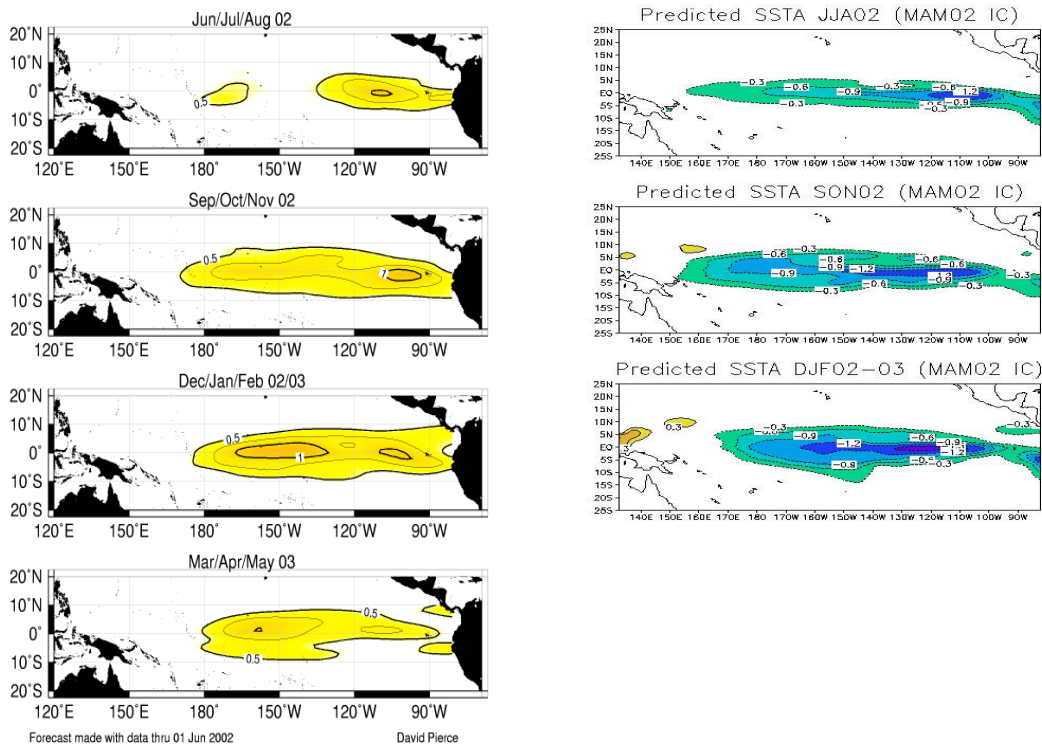


Figure 15: Two recent seasonal forecasts taken from the COLA Experimental Long-Lead Forecast Bulletin. What are we going to do with such a kind of forecasting situation? Left: Scripps HCM, Right: Kirtman model.

7 Summary

We have discussed several new theoretical concepts that might help to generate appropriate ensembles for seasonal forecasting.

Still important challenges have to be tackled as the one shown in **Figure 15**.

Acknowledgements: A.T. wishes to thank his friend R.A. Pasmanter for a wonderful collaboration on the topics of climate prediction and ENSO dynamics.

8 References

- An. S.I., and F.-F. Jin, 2000: An Eigen analysis of the interdecadal changes in the structure and frequency of the ENSO mode, *Geophys. Res. Lett.*, 27, 2573-2576.
- Arnéodo, J. Elzgaray, J. Pearson, T. Russo, 1991: Instabilities of front patterns in reacting-diffusion systems, *Physica D* 49, 141-160.
- Aurell, E. et al. 1997 : Predictability in the large : an extension of the concept of Lyapunov exponent, *J. Phys.*, A 30, 1.
- Bofetta, G., P. Giuliani, G. Paladin, and A. Vulpiani, 1998: An extension of the Lyapunov analysis for the

predictability problem. *Journal of the Atmospheric Sciences* 55, 3409-3416.

Breiman, L. and Friedman, J. H. 1985: Estimating Optimal Transformations for Multiple Regression and Correlation. (with discussion) *J. Amer. Statist. Assoc.* 80, 580.

Burgers, G., 1999: The El Niño Stochastic Oscillator, *Clim. Dyn.* 15, 491-502.

Burgers, G., D.B. Stephenson, 1999: The normality of El Niño, *Geophys. Res. Lett.*, 26, 1027-1030.

Casdagli, M., 1989: Nonlinear Prediction of Chaotic Time Series. *Physica D*, 35, 335-356.

Chen, Y-Q. et al.. 1995 : A study of the predictability of tropical Pacific SST in a coupled atmosphere-ocean model using singular vector analysis : the role of the annual cycle and the ENSO cycle, *Mon. Wea. Rev.* 125, 831-845.

Eckert, C., 1999: On the predictability limits of ENSO. A study performed with a simplified model of the tropical Pacific ocean-atmosphere system, Examsarbeit Nr. 55, 76pp., [available from the Max Planck Institut für Meteorologie, Bundesstr.55, D-20146 Hamburg, Germany].

Farrell, B.F., and P.J. Ioannou, 1996: Generalized Stability Theory. Part I: Autonomous operators, *J. Atmosph. Sciences*, 53, 2025-2040.

Gill, A., 1980: Some simple solution for the heat-induced tropical circulation, *Q.J.R. Meteorol. Soc.*, 106, 447-462.

Grötzner, A., M. Latif, A. Timmermann, R. Voss, 1999: Interannual to Decadal Predictability in a Coupled Ocean-Atmosphere General Circulation Model. *Journal of Climate*, 12, 2607-2624.

Haken, H., *Synergetics, An Introduction*, 2nd ed. (Springer, Berlin, Heidelberg, New York), 1978.

Hegger, R., Kantz, H., Schreiber, T., 1999: Practical implementation of nonlinear time series methods: The TISEAN package. *Chaos*, 9, 413.

Hendon, H.H, J. Glick, 1997: Intra-seasonal air-sea interactions in the tropical Indian and Pacific Oceans, *J. Climate*, 10, 647-661.

Jin, F.-F., 1997: An equatorial ocean recharge paradigm for ENSO. Part I: Conceptual model, *J. Atmos. Sci.* 54, 811.

Jin, F.-F. S.I. An, A. Timmermann, 2002: Linkages between El Niño and Recent Tropical Warming, submitted to *Science*.

Kleeman, R. 1991: A simple model of the atmospheric response to ENSO Sea Surface Temperature Anomalies, *J. Atmos. Sci.*, 48, 3-18.

Kleeman R. and A.M. Moore, 1997, : A theory for the limitation of ENSO predictability due to stochastic atmospheric transients, *Journal of Atmos. Sci.*, Vol 54, pp753-767.

Landsea,C.W., Knaff,J.A., 2000: How much skill was there in forecasting the very strong 1997-98 El Nino?, *Bulletin of the American Meteorological Society*, v.81, pp.2107-2119.

Lorenz, E.N., 1963: Deterministic non-periodic flow, *J. Atmosph. Sci.*, 20, 130.

Lorenz, E.N., 1969: The predictability of a flow which possesses many scales of motion, *Tellus*, 21, 289.

Lorenz, E.N. Climate Predictability. In: *The Physical Bases of Climate and Climate Modeling*, number 16 in GARP Publ. Ser., pages 132-136. World Meteorol. Org., 1975.

Metzger, S. M., M. Latif, and K. Fraedrich, 2001: Combining ENSO - Forecasts: A Feasibility Study. *J Climate*, submitted.

Moore, A.M. and R. Kleeman, 1997: The singular vectors of a coupled atmosphere-ocean model of ENSO. *Quart. J. Roy. Met. Soc.*, 123, 953-981.

Moore A.M. and R. Kleeman, 1999: Stochastic Forcing of ENSO by the intraseasonal oscillation, *J. Clim.*, Vol 12, 1199-1220.

Pasmanter, R.A., and A. Timmermann, 2002: Cyclic Markov Chains with an Application to an intermediate ENSO model, *Nonl. Proc. in Geophysics*, accepted.

Stockdale, T.N., D.L.T. Anderson, J.O.S. Alves and M.A. Balmsadea, 1998: Global seasonal rainfall forecasts using a coupled ocean-atmosphere model, *Nature*, 392, 370-373.

Syu, H.-H., J.D. Neelin, ENSO in a hybrid coupled model, Part I: sensitivity to physical parametrizations, *Climate Dynamics*, 16, 19-34.

Timmermann, A., M. Latif, A. Bacher, J. Oberhuber, E. Roeckner, 1999: Increased El Niño frequency in a climate model forced by future greenhouse warming, *Nature*, 398, 694-696.

Timmermann, A., M. Latif, R. Voss, 1999a: Modes of Climate Variability as simulated by the coupled atmosphere-ocean model ECHAM3/LSG, Part I: ENSO-like climate variability and its low-frequency modulation, *Clim. Dyn.*, 15, 605-618.

Timmermann, A., H. Voss, R. Pasmanter, 2001. Empirical Dynamical System Modeling of ENSO using Non-linear Inverse Techniques, *J. Phys. Oceanogr.*, 31, 1579-1598.

Timmermann, A. 2002, Decadal ENSO Amplitude Modulations: A Nonlinear Mechanism, *Global and Planetary Changes*, in press.

Timmermann, A. F.-F. Jin, J. Abshagen, 2002: A nonlinear Theory for ENSO Bursting. *Journal of The Atmosph. Sciences*, in press.

Torrence, C. and G. P. Compo, 1998: A practical guide to wavelet analysis. *Bull. Amer. Meteor. Soc.*, 79, 61-78.

Trefethen, L.N., A.E. Trefethen, S.C. Reddy and T.A. Driscoll, 1993: Hydrodynamic stability without eigenvalues, *Science*, 261, 578-584.

Voss, H. and J. Kurths, 1997: Reconstruction of nonlinear time delay models from data by the use of optimal transformations, *Physics Letters A* 234, 336-344.

Voss, H.U., 2001: Analyzing Nonlinear Dynamical Systems with Nonparametric Regression, in: A.I. Mees (ed.), *Nonlinear Dynamics and Statistics*, p. 413-434, Birkhäuser, Boston.

Zebiak, S. and M.Cane, 1987: A model of the El Niño-Southern Oscillation, *Mon. Wea. Rev.*, 115, 2262-2278.